SEISMIC PERFORMANCE AND DESIGN DETAILS OF LOW-RISE STEEL STRUCTURES EQUIPPED WITH THE SEESAW SYSTEM

D. Beskos[(1)], P. Katsimpini[(2)], G. Papagiannopoulos[(3)], D. Karabalis[(4)], G. Hatzigeorgiou[(5)]

[(1)] *Professor, Department of Disaster Mitigation for Structures, College of Civil Engineering, Tongji University, dimisof@hotmail.com*
[(2)] *Ph.D candidate, Department of Civil Engineering, University of Patras, penyk@hotmail.gr*
[(3)] *Instructor, School of Science and Technology, Hellenic Open University, papagiannopoulos.georgios@ac.eap.gr*
[(4)] *Professor, Department of Civil Engineering, University of Patras, karabali@upatras.gr*
[(5)] *Professor, School of Science and Technology, Hellenic Open University, hatzigeorgiou@eap.gr*

Abstract

The seismic performance of three-dimensional low-rise steel structures equipped with the seesaw system is evaluated on the basis of response results coming from nonlinear time-history seismic analyses. The response results involve maximum interstorey drift ratios (temporary and residual), plastic hinge formations to steel beams and columns as well as peak forces to spiral strand ropes (cables) and viscous dampers of the seesaw system. The steel structures are simultaneously subjected to the two horizontal components of twenty four recorded seismic motions taking into account the orientation of seismic incident angle. The structures are assumed to be founded either on firm or on compliant ground in order to assess the effects of soil-structure interaction (SSI). Some key analysis/design issues regarding the structural implementation of the seesaw system, i.e., its placement concentrically or eccentrically with respect to perimeter steel frames are discussed. Pertinent design details of the seesaw system are also provided. It is concluded that the seesaw system effectively controls the seismic performance of low-rise steel structures and can be adopted by seismic codes as an alternative seismic force resisting system.

Keywords: seesaw system; steel structures; seismic performance; design details

1. Introduction

The seesaw system constitutes a recent innovative seismic force resisting system for steel structures and its original analytical and experimental applications can be found in [1-4]. The noticeable seismic response and damping capacity features of the seesaw system when used in 2-D steel frames have been highlighted in [5]. In this work a study and its results regarding the seismic performance of low-rise 3-D steel structures equipped with the seesaw are presented and some key issues regarding the structural implementation of the seesaw system, i.e., its concentric or eccentric placement with respect to perimeter steel frames, as well as design details of the seesaw members are discussed.

A typical seesaw system installed in a steel frame, as shown in Fig.1, consists of a pin-supported seesaw, two spiral strand ropes (cables) properly adjusted by turnbuckles and cross turnbuckles as well as a couple of dampers installed vertically on the seesaw. The spiral strand ropes are anchored via fork end connectors secured with pins to the seesaw and to gusset plates that are welded to the beam-to-column connection. The spiral strand ropes of the seesaw system are always in tension and some pretension is introduced to them in order to ensure their immediate activation at initiation and first reversals of seismic motion [5,6].

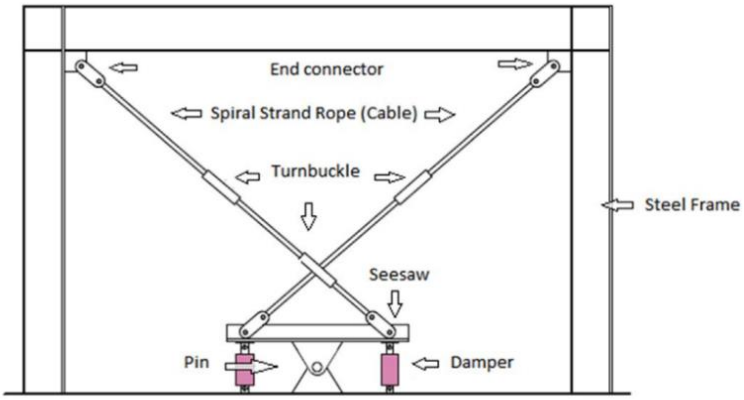

Fig. 1 – A steel frame equipped with the seesaw system

In the following, some seismic response results involving 2-, 5- and 8-storey steel structures equipped with the seesaw system are presented. These seismic response results have been obtained by non-linear time history analyses of the steel structures, employing simultaneously the two horizontal components of twenty four recorded seismic motions and varying the angle of seismic incidence. The seismic response results involve maximum interstorey drift ratio (IDR) and residual drift ratio (RIDR), plastic hinge formations to beams and columns of the steel structures as well as peak forces to spiral strand ropes and viscous dampers of the seesaw system. Failure of the spiral strand ropes and of the linear viscous dampers of the seesaw system is also checked. The steel structures are assumed to be founded either on firm or on compliant ground in order to assess the effects of soil-structure interaction (SSI) on the aforementioned seismic response results. The concentric or eccentric placement of the seesaw system with respect to perimeter frames is discussed in view of the computed seismic drifts and plastic hinge formations in beams and columns of the steel structures. Finally, indicative design details of the seesaw system are provided taking into account that for the case of its concentric placement, the spiral strand ropes have to pass through beams and columns.

It is thus demonstrated that the seesaw system can be applied in praxis no matter if architectural restrictions enforce its concentric or eccentric placement with respect to perimeter frames of a steel structure. Overall, it can be said that the seesaw system constitutes an attractive and reliable bracing solution for steel structures. It comes naturally to say that the spiral strand ropes of the seesaw system, being always in tension, do not face any of the buckling issues associated with common steel braces.

2. Seismic analysis of steel structures equipped with the seesaw system

The 2-, 5- and 8-storey 3-D steel structures studied are shown in Fig.2, where the seesaw system (its spiral strand ropes are shown with green colour) is installed at the middle bay of the perimeter frames. The spiral strand ropes emanating from the seesaw device (see Fig.1) are anchored at both ends of the perimeter beams and at the same floor level. On the basis of Fig.2, the number of seesaw systems in the 2-, 5- and 8-storey 3-D steel structures is 4, 4 and 8, respectively. There is no eccentricity of any of these seesaw systems with respect to the perimeter frame where they are installed. Slotted holes are assumed to exist at the flanges of some beams and columns so that the spiral strand ropes can pass through them.

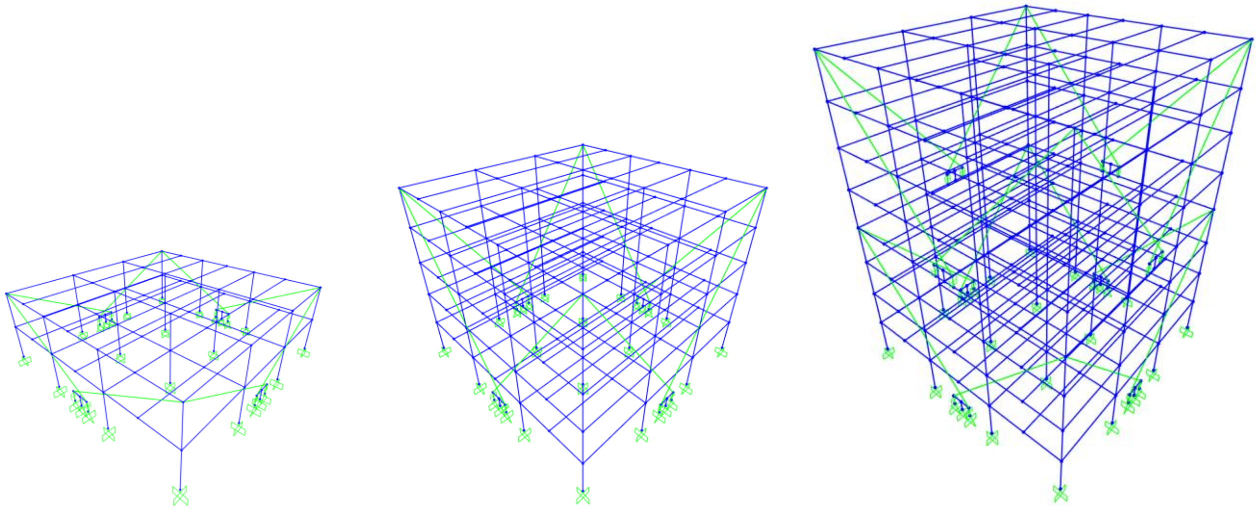

Fig. 2 – 2-, 5- and 8-storey steel structures equipped with the seesaw system

The steel structures shown in Fig.2 have a square plan configuration of 18.0x18.0m, storey heights of 3.0m and bay spacing of 6.0m in each direction. The orientation of steel columns is shown in Fig.3. Diaphragm action is assumed at every floor due to the presence of a composite slab. Dead and live loads on the composite slabs are 8.0kN/m^2 and 3.0kN/m^2, respectively. The steel structures are initially designed as typical concentrically braced frames according to EC3 [6] and EC8 [7] with fixed base. The design seismic load is calculated using the design spectrum of EC8 [7] that corresponds to peak ground acceleration (PGA) of 0.36 g, soil type B and behaviour factor equal to 3. The storey shear computed from spectrum analysis is used in order to estimate the diameter of the spiral strand ropes of the seesaw system. Effects of accidental torsion are omitted. The stability coefficient is computed at every storey of the steel structures and it is checked according to EC8 [7].

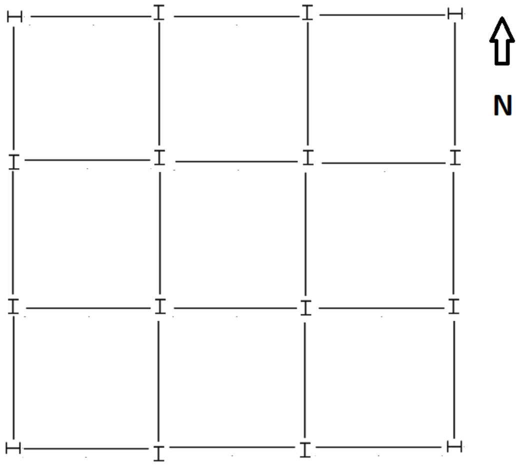

Fig. 3 – Orientation of steel columns for steel structures of Fig.2

Pretension is applied to the spiral strand ropes (about 5-10% of their tensile breaking strength) and it is also assumed that their anchorage type is such that the tensile breaking strength values do not need to be reduced [8]. Vertically positioned linear viscous dampers (in a clevis-clevis configuration) with a damping coefficient of 250kNs/m are utilized. Due to the mid-stroke length of these dampers, the height of the vertical steel plates of the seesaw is 870mm. The length of the horizontal steel plate of the seesaw is 1600mm. The width of the horizontal plate of the seesaw is equal to the height of the section of the column or to the width of the flange of the column, depending on the orientation of the column (Fig.3).

The steel grade used is S235 for beams and S355 for columns and seesaw plates. All connections of steel members are moment-resisting ones except those of the secondary beams (interior beams at floor levels that are not part of a frame as shown in Fig.2) that are pinned. The design of the steel structures of Fig.2 is performed by SAP 2000 [9]. Final sections for columns, beams and for the diameter and the design tensile breaking strength of the spiral strand ropes are presented in Table 1. Referring to Figs.2-3, the same diameter of spiral strand ropes is used in both horizontal directions of the steel structures.

Table 1 – Sections of beams & columns, diameter and design breaking strength of the spiral strand ropes

Steel structure	Beams	Columns	Diameter (mm)	Breaking strength (kN)
2-storey	IPE 450	HEM 320	50	1560
5-storey	IPE 500	HEM 600	110	7570
8-storey	IPE 500	HEM 700	115	8270

Considering the steel structures of Fig.2. to be founded either on firm ground (soil type B) or on compliant ground (soil types C & D), a 20.0x20.0m rigid mat foundation is designed with depth 0.3m, 0.6m and 0.8m for the 2-, 5- and 8-storey steel structures, respectively. SSI is taken into account for soil types C and D, while its effect is considered to be negligible for soil type B and, thus, it is ignored. Thus, the steel structures of Fig.2 when founded on soil type B, are assumed to be fixed base. SSI is considered in seismic analyses via a 3-D discrete system of frequency independent springs, dashpots and masses which effectively replace the mat foundation and its surrounding soil, as reported in [10]. Only one such discrete system is needed to model a rigid mat foundation.

The values for the springs, dashpots and masses of this discrete system are calculated utilizing the formulas provided in [10]. These values correspond to linear soil behavior but can be turned into equivalent linear ones following the recommendations of EC8 [7] in consideration of the anticipated soil nonlinearity at strong ground motions. Therefore, the shear modulus of soil types C and D is initially obtained using a shear wave velocity equal to 270m/sec and 180m/sec and a soil density equal to 1800kgr/m^3 and 1900kgr/m^3, respectively, and it is then conservatively reduced to 16% of its initial value in order to take into account the development of non-linear soil deformations in soil types C and D for large levels of ground acceleration. Due to the aforementioned reduction of the shear modulus of soil types C and D, the shear wave velocity of these soil types is less than 100m/sec, which is in accordance to the SSI consideration requirement of EC8 [7].

Employing the aforementioned discrete system that simulates SSI, the steel structures of Fig.2 are dimensioned for the design spectrum of EC8 [7] and soil types C and D, with PGA 0.36g and behavior factor q=3. The geometric properties of the steel structures founded on soil types C and D are the same as those in Table 1 (corresponding to soil type B), even though the stress ratio of some sections is greater for the case of soil type D than those for soils B and C.

The steel structures shown in Fig.2 are then subjected simultaneously to the two horizontal components of the 24 seismic motions presented in Table 2. In this table additional details pertaining to location, date, recording station, moment magnitude M_w and soil type, can also be found. Regarding the soil type, the abbreviations HR, SR and SL correspond to hard rock, sedimentary and conglomerate rock, and soil/alluvium, respectively. Neither amplitude scaling nor spectral matching procedures are applied to the seismic motions of Table 2 as well as to the determination of their critical orientation. Thus, the seismic motions of Table 2 maintain their as-recorded orientation and are applied in the direction of the two orthogonal structural axes of Fig.3 considering three values for the horizontal angle of seismic incidence, i.e., 0°, 45° and 90°, with respect to the geometric center of the column layout.

Table 2 – Seismic ground motions

No.	Earthquake, Location	Date	Recording Station	M_w	Soil type
1.	San Fernando, U.S.A.	09/02/1971	Pacoima Dam	6.6	HR
2.	Imperial Valley, U.S.A.	15/10/1979	El Centro Array 6	6.5	SL
3.	Valparaiso, Chile	03/03/1985	Llolleo	7.9	SR
4.	Michoachan, Mexico	19/09/1985	SCT	8.0	SL
5.	Vrancea, Romania	30/08/1986	INCERC	7.3	SL
6.	Superstition Hills, U.S.A.	24/11/1987	Parachute Test Site	6.5	SL
7.	Loma Prieta, U.S.A.	17/10/1989	Los Gatos	7.0	HR
8.	Cape Mendocino, U.S.A.	25/04/1992	Cape Mendocino	6.9	SR
9.	Cape Mendocino, U.S.A.	25/04/1992	Petrolia	6.9	SR
10.	Landers, U.S.A.	28/06/1992	Lucerne Valley	7.3	SL
11.	Northridge, U.S.A.	17/01/1994	Rinaldi Receiving St.	6.7	SL
12.	Northridge, U.S.A.	17/01/1994	Newhall	6.7	SL
13.	Northridge, U.S.A.	17/01/1994	Sylmar Converter St.	6.7	SL
14.	Kobe, Japan	17/01/1995	Takatori	6.9	SL
15.	Chi-Chi, Taiwan	20/09/1999	TCU 052	7.6	SL
16.	El Salvador, El Salvador	13/01/2001	Observatorio	7.6	SR
17.	Denali, Alaska	03/11/2002	Taps Pump station 10	7.9	SR
18.	Bam, Iran	26/12/2003	Bam	6.5	SL
19.	Ica Pisca, Peru	15/08/2007	ICA2	8.0	SL
20.	Maule, Chile	27/02/2010	Constitution	8.8	SR
21.	Darfield, New Zealand	03/09/2010	Greendale	7.0	SL
22.	Christchurch, New Zealand	22/02/2011	Lyttelton Port Company	6.3	SL
23.	Christchurch, New Zealand	22/02/2011	Resthaven	6.3	SL
24.	Kefalonia, Lixouri	03/02/2014	Lixouri	6.1	SR

The seismic response of the steel structures shown in Fig.2 is determined through non-linear time-history analyses using SAP 2000 [9]. Geometrical non-linearities are also taken into account. Beams and columns are modelled using standard frame elements with concentrated plasticity and 2% strain hardening. Plastic hinges in beams are formed due to uniaxial bending, whereas those in columns due to interaction of axial force-biaxial bending. The limits for plastic hinge rotations for the frame members follow ASCE 41-17 [11]. The internal viscous damping of the steel structure is considered to be 3%. The constants of the Rayleigh damping matrix are then defined utilizing the fundamental period of the structure and the period of its highest mode of significance. Diaphragm action is assumed at every floor due to the presence of the composite slab. Linear viscous dampers are modelled as discrete damping elements using the 'Link element' option [9]. The horizontal and vertical steel plates of the seesaw are modelled as rigid elements, whereas the spiral strand ropes are modelled as cable elements considering geometrical non-linearities and pretension. The 'Link element' [9] is also employed to model the discrete system of springs, dashpots and masses [10] in order to capture the effects of SSI. The non-linear time-history seismic analyses are firstly conducted for fixed base steel structures where SSI is absent, and then for steel structures founded on soil types C or D where SSI is present.

3. Seismic response results

The seismic response results presented in this section involve maximum IDRs and RIDRs, worst (taking into account the ensemble of the seismic analyses performed) plastic hinge formations in frame elements as well as peak forces to spiral strand ropes. The characterization of worst plastic hinge formations is based on the number of frame elements in which plastic hinges occur as well as on the level of plastic hinge rotation [9, 11]. In all seismic analyses performed the linear viscous dampers do not fail, i.e., their maximum stroke or maximum force is not surpassed. For those analysis cases that either the threshold value of 0.5% for RIDR or the design tensile strength of the spiral strand ropes is surpassed, response results are discarded. For the rest of the analyses, response results are processed and one observes the following: i) plastic hinge rotations of frame members are found to be either below the limit value of IO (Immediate Occupancy) level or between those of the IO and LS (Life Safety) levels, while the limit value of the LS level is never exceeded and ii) soft-storey mechanisms do not occur. For reasons of performing comparison per structure, maximum values for IDR, RIDR and force to spiral strand ropes (cables) are discussed in the following on the basis of fixed or compliant (soil types C & D) base conditions and the angle of seismic incidence.

Starting with the 2-storey structure, from the plots shown in Fig.4, one observes that: i) maximum values for IDR and RIDR are found for the case of soil type D and 0° angle of seismic incidence; ii) maximum force to spiral strand ropes is found for the case of 0° incidence angle and soil types C, D; iii) 0° is the angle of seismic incidence that produces maximum IDR, RIDR and force to spiral strand ropes for the case of soil types C; iv) in the case of fixed base conditions, maximum values for IDR, RIDR, force to spiral strand ropes are obtained for different angles of seismic incidence; v) the worst case of plastic hinge formation corresponds to soil type C and 90° incidence angle, where the expected damage to frame elements is either below to the limit value of the LS level or below to that of the IO level.

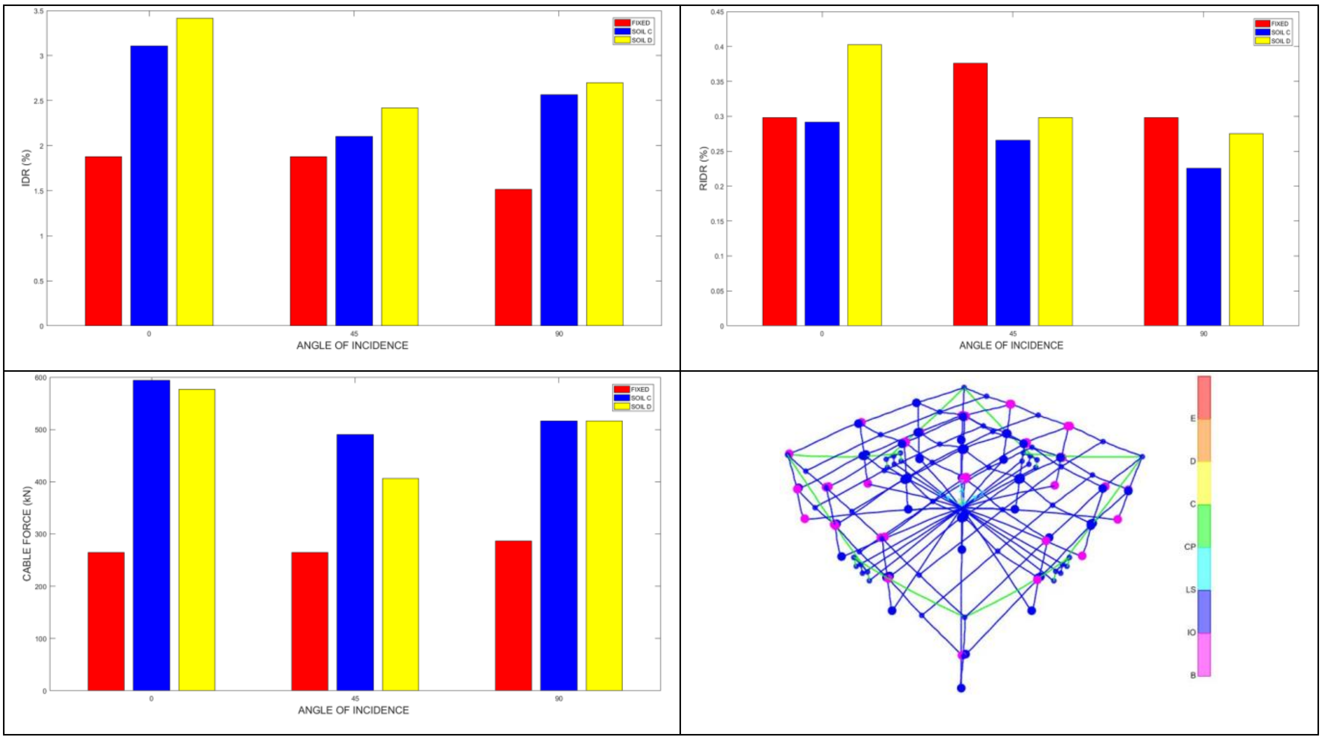

Fig. 4 – Seismic response results for the 2-storey steel structures

Moving to the 5-storey structure, from the plots shown in Fig.5, one observes that: i) maximum values for IDR and RIDR are found for the case of soil type D and for 0° and 45°incidence angles, respectively; ii) maximum force to spiral strand ropes is found for the case of 0° incidence angle and soil type D; iii) 0° is the angle of seismic incidence that produces maximum IDR, force to spiral strand ropes for the case of soil types C and D and maximum RIDR for the case of soil C. Maximum RIDR for soil type D is found for an incidence angle of 45°; iv) in the case of fixed base conditions, maximum IDR and RIDR values are found for 90° incidence angle, whereas peak force to spiral strand ropes is found for 0° incidence angle; v) the worst case of plastic hinge formation corresponds to fixed base and 90° incidence angle, where the expected damage to frame elements is either below to the limit value of the LS level or below to that of the IO level.

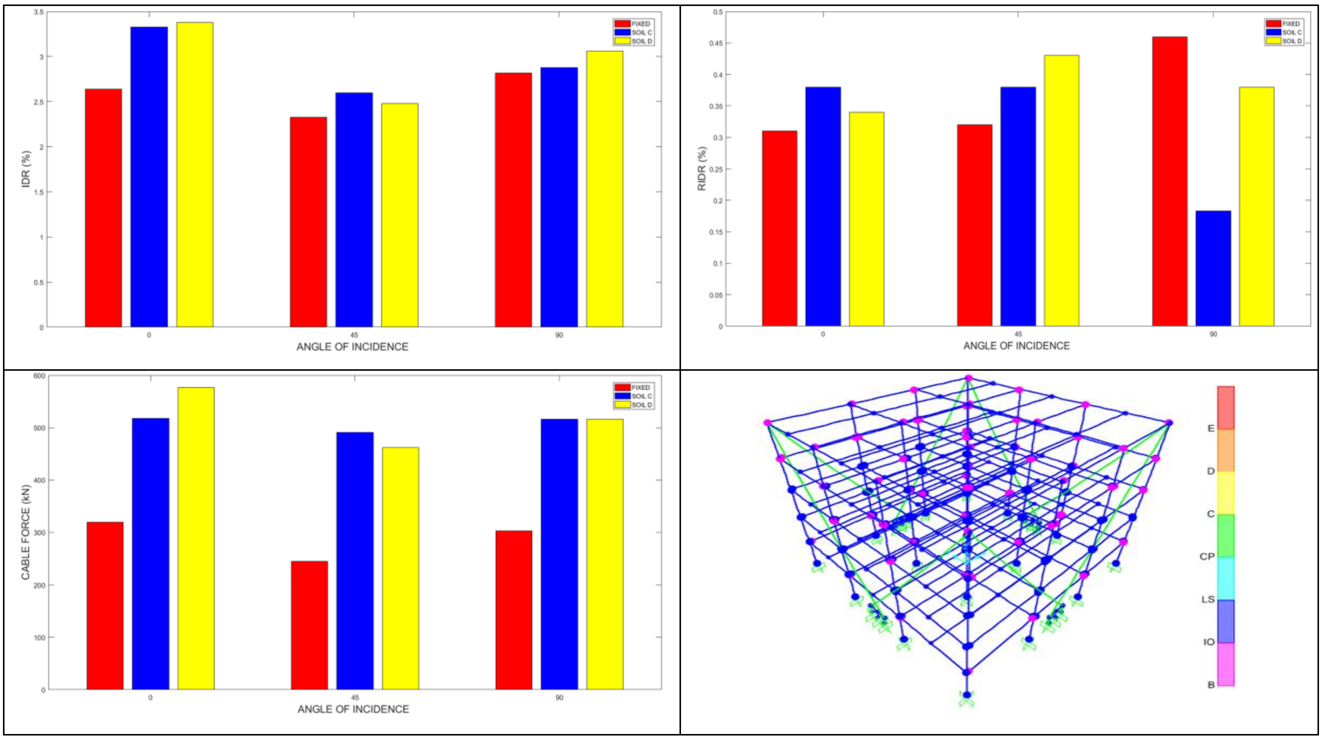

Fig. 5 – Seismic response results for the 5-storey steel structures

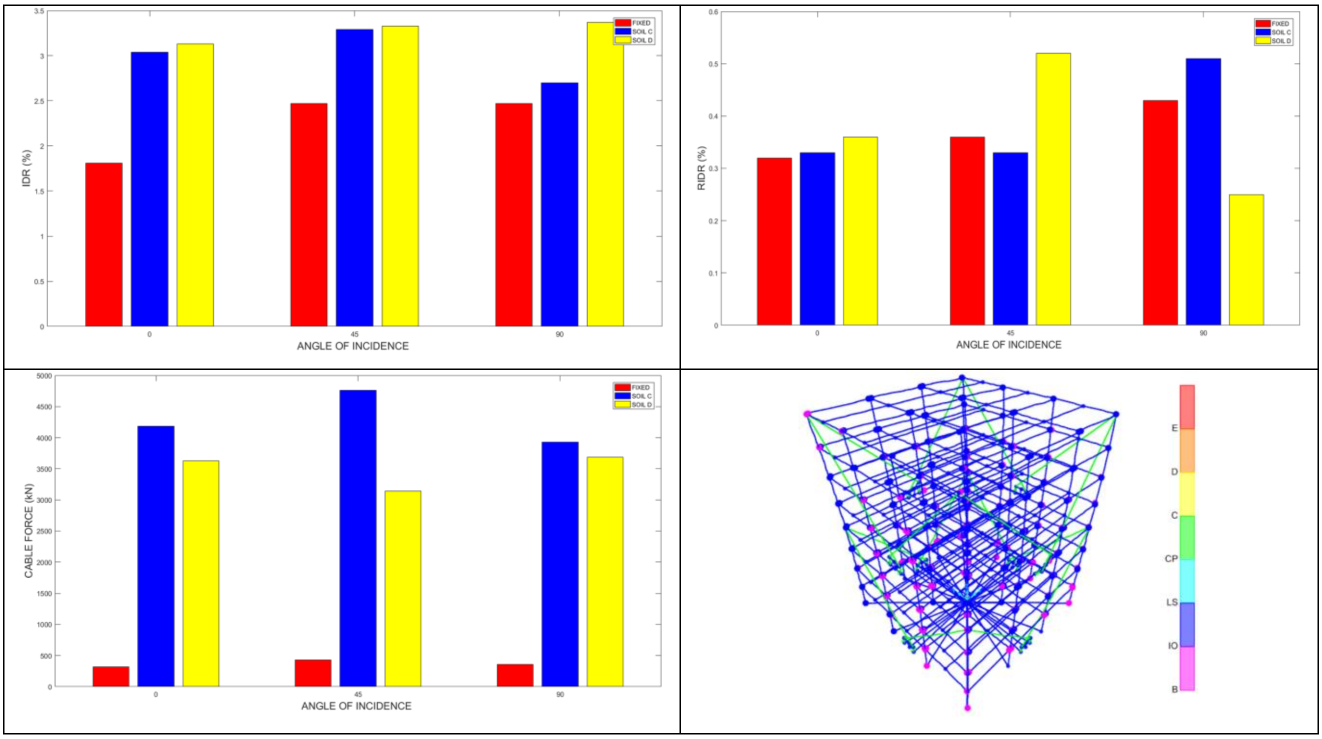

Fig. 6 – Seismic response results for the 8-storey steel structures

Finally, from the plots shown in Fig.6 that correspond to the 8-storey structure, one observes that: i) maximum values for IDR and RIDR are found for the case of soil type D and for 90° and 45° incidence angles, respectively; ii) maximum force to spiral strand ropes is found for the case of 45° incidence angle and soil type C; iii) in the case of soil type D, maximum values for IDR, RIDR and force to spiral strand ropes are obtained for different angles of seismic incidence; iv) in the case of soil type C, maximum IDR and force to spiral strand ropes are found for 45° incidence angle, whereas maximum values for RIDR are found for 90° incidence angle; v) in the case of fixed base conditions, maximum values for IDR and force to spiral strand ropes are found for 45° incidence angle, whereas maximum RIDR value is found for 90° incidence angle; vi) the worst case of plastic hinge formation corresponds to soil type D and 90° incidence angle, where the expected damage to a large number of frame elements is below to the limit value of the LS level and to fewer frame elements is below to that of the IO level. It should be noted that maximum force to spiral strand ropes of the 8-storey structure are notably higher for the cases of soil types C and D in comparison to those corresponding to the case of fixed-base conditions. However, the peak force to spiral strand ropes is within its design value (Table 1).

4. On the structural implementation of the seesaw system

Cutouts in the form of slotted holes have to be performed to beams and columns of the perimeter frames for the placement of the seesaw system according to Fig.2. Therefore, it is of interest to investigate other possible configurations for the seesaw system where cutouts are either reduced or are not needed. Considering that the seesaw device remains concentrically placed in the middle bay of the perimeter frames of the steel structures of Fig.2, there are two more configurations of the seesaw system possible. These configurations are shown in Fig.7 only for the case of 2-storey steel structures but can be also adopted for the 5- and 8-storey structures studied herein. In particular: i) the spiral strand ropes (shown with green color) are anchored at both ends of the middle perimeter beam and at the same floor level (Fig.7, left). Thus, there is one seesaw device per floor and side of the perimeter; ii) the spiral strand ropes (shown with green color) are anchored at both ends of the middle perimeter beam of the upper storey (Fig.7, right). Therefore, for configuration i) no cutouts are needed, whereas for configuration ii) cutouts are needed at the flanges of the beam of the first storey. It is recalled that the common characteristic among the seesaw configurations presented in Figs.2 and 7 is their concentric placement with respect to the perimeter frames.

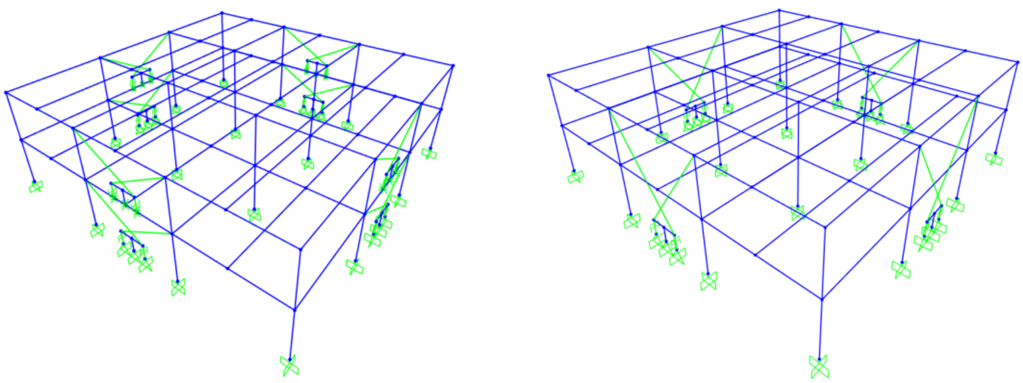

Fig. 7 – Alternative placements of the seesaw system for the 2-storey steel structure

The choice behind the selection of the most appropriate configuration of the seesaw system, when it is concentrically placed with respect to the perimeter frames, depends not only on the number of seesaw devices used and of steel member cutouts performed but also on the expected seismic drifts and plastic hinge formations to steel members. Employing the seismic motions of Table 2 in the context of non-linear time history analysis involving the 2-storey steel structures of Fig.7, it is concluded that for the seesaw configurations i) and ii), similar seismic behavior to that of the default seesaw configuration shown in Fig.2 may be achieved. That is the maximum values for IDR, RIDR and force to spiral strand ropes as well as the number plastic hinge formations and their associate rotation are in close accordance with those presented in

Fig.4. However, the number of seismic motions for which either the threshold value of 0.5% for RIDR or the design tensile strength of the spiral strand ropes is surpassed, is greater for seesaw configurations i) and ii) of Fig.7 in comparison with the default seesaw configuration of Fig.2. In fact, seesaw configuration ii) is marginally better than i). Similar conclusions can be reached for the case of 5- and 8-storey steel structures when seesaw configurations i) or ii) are to be compared with the default seesaw configuration of Fig.2.

A somehow different placement of the seesaw system, essentially motivated by [12], is presented in Fig.8 for the case of 2-storey steel structure but can be also adopted for the 5- and 8-storey structures studied herein. As Fig.8 displays, the seesaw system is implemented eccentrically with respect to the perimeter frames. The spiral strand ropes (shown with green color) of the seesaw system do not pass through beams or columns and they are anchored to short cantilevers of about 500mm length. These short cantilevers of square or rectangular hollow section have been properly detailed on the top of the four edge columns (according to column layout of Fig.2) and in both horizontal directions.

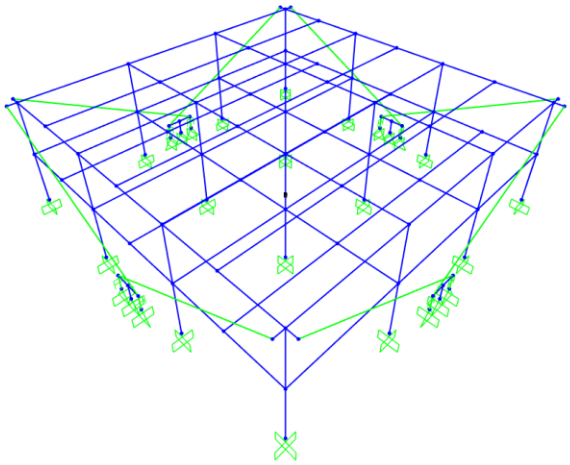

Fig. 8 – Eccentric placement of the seesaw system for the 2-storey steel structure

Leaving aside any issue related to architectural restrictions, the selection of the seesaw placement as shown in Fig.8 is a matter of taking properly into account: i) the effects of the eccentricity of the seesaw members to the steel structure; ii) the design of the cantilever beams and their connections against the combined effect of torsion, biaxial shear and biaxial moment; iii) the number of the seesaw devices that can be actually placed.

Regarding the maximum seismic drifts and force to spiral strand ropes as well as plastic hinge formations to steel members, non-linear time-history analyses of the 2-storey steel structure of Fig.8 employing the seismic motions of Table 2 reveal similar seismic behavior to that of the default seesaw configuration of Fig.2. In fact, maximum values for IDR, RIDR and force to spiral strand ropes as well as the number plastic hinge formations and their associate rotations can be even lower than the corresponding ones presented in Fig.4. The same conclusions can be reached for the case of 5- and 8-storey steel structures when the seesaw placements of Fig.2 and 8 are compared. One last thing to note is that for the case of the 8-storey steel structure, the seesaw device at the middle bay of the perimeter beam of the fourth floor (Fig.2) in order to be eccentrically placed in the form of Fig.8, it has to be supported by a system of short cantilevers.

5. Design details

To demonstrate the practical application of the seesaw system, indicative design details are presented in this section. Figures 9 and 10 provide the design details needed for the concentric implementation of the seesaw system to the steel structures of Fig.2 along the EW and NS directions, respectively, following the orientation shown in Fig.3. These design details satisfy all pertinent requirements in [13-15].

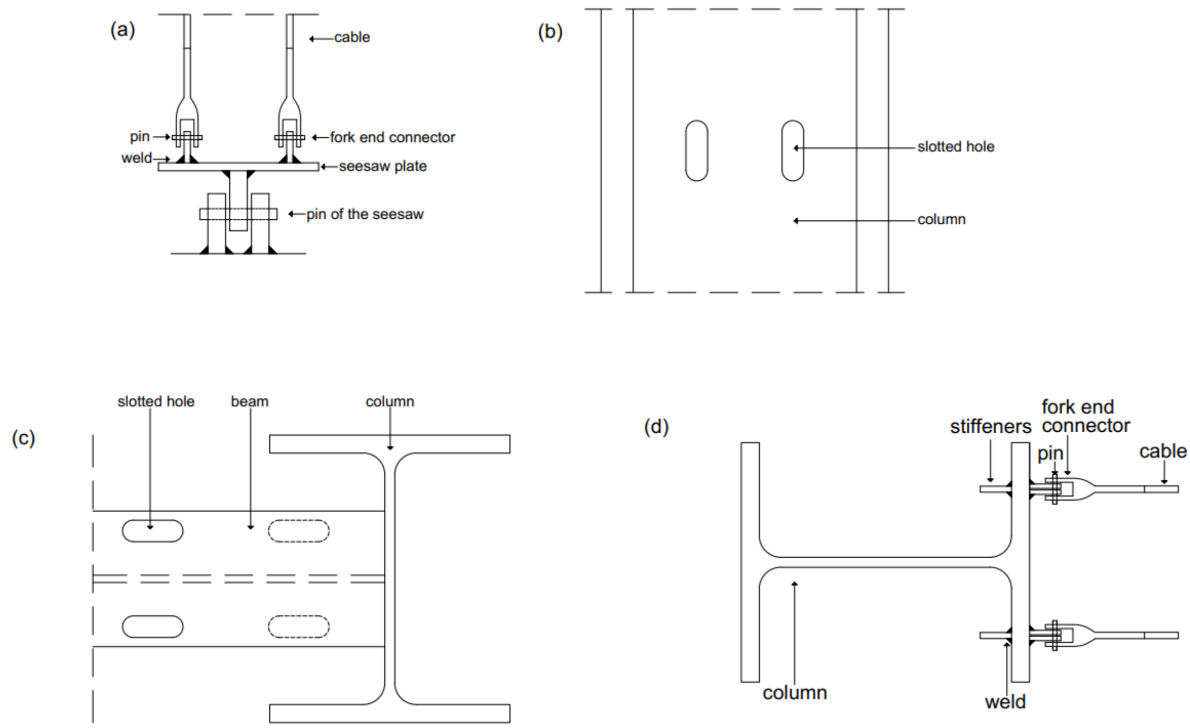

Fig. 9 – Design details for the implementation of the seesaw system along EW direction shown in Fig.3

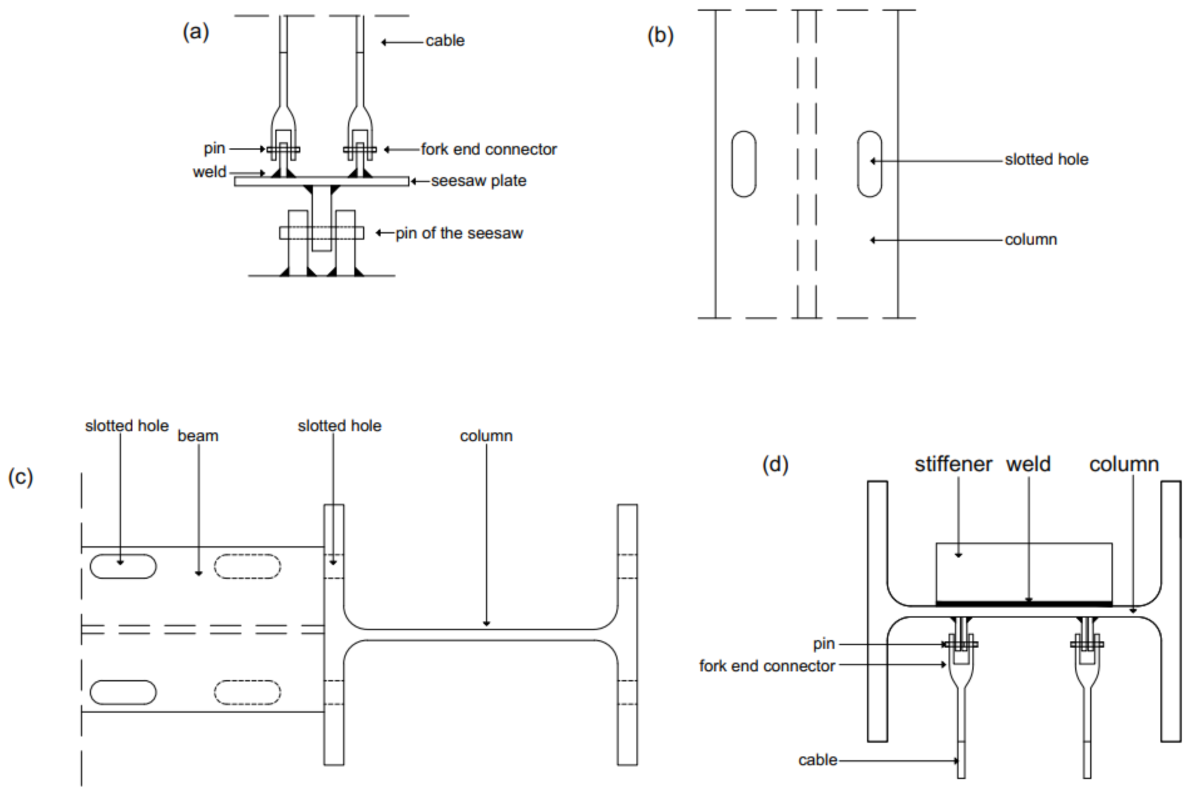

Fig. 10 – Design details for the implementation of the seesaw system along NS direction shown in Fig.3

In particular, the details shown in Figs.9-10 have as follows: detail (a) displays the plate of the seesaw supported by a pin connection. Cables (spiral strand ropes) are anchored to the seesaw plate by fork end connectors; details (b) and (c) display the slotted holes performed on the web or on the flanges of the column and on the flanges of the beams, so that cables can pass through them; (d) displays the anchorage of the cables either on the flange or on the web of the column by fork end connectors. Welds and stiffeners are also shown where needed. Special stiffeners should be provided in the immediate regions of the slotted holes and are shown as details (a) and (b) in Fig.11. Detail (c) in Fig.11 displays the cross turnbuckle or cross coupler needed when two cables that emanate from the seesaw device intersect.

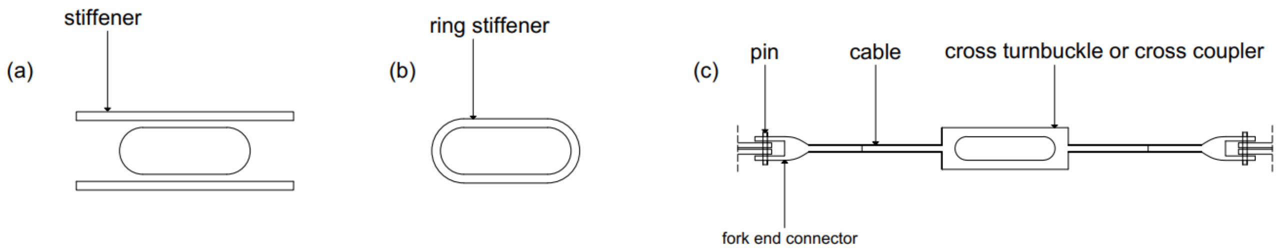

Fig. 11 – Stiffeners to reinforce slotted holes and turnbuckle needed for the intersection of cables

Finally, Fig.12 presents the details of the eccentric placement of the seesaw system (Fig.8), i.e., the short cantilever connected to the flange or to the web of the column (details (a) and (b)) and the anchorage of the cables on the vertical side of the short cantilever (detail (c)). The basic welds are also shown in details (a)-(c), whereas additional welds and stiffeners may be needed.

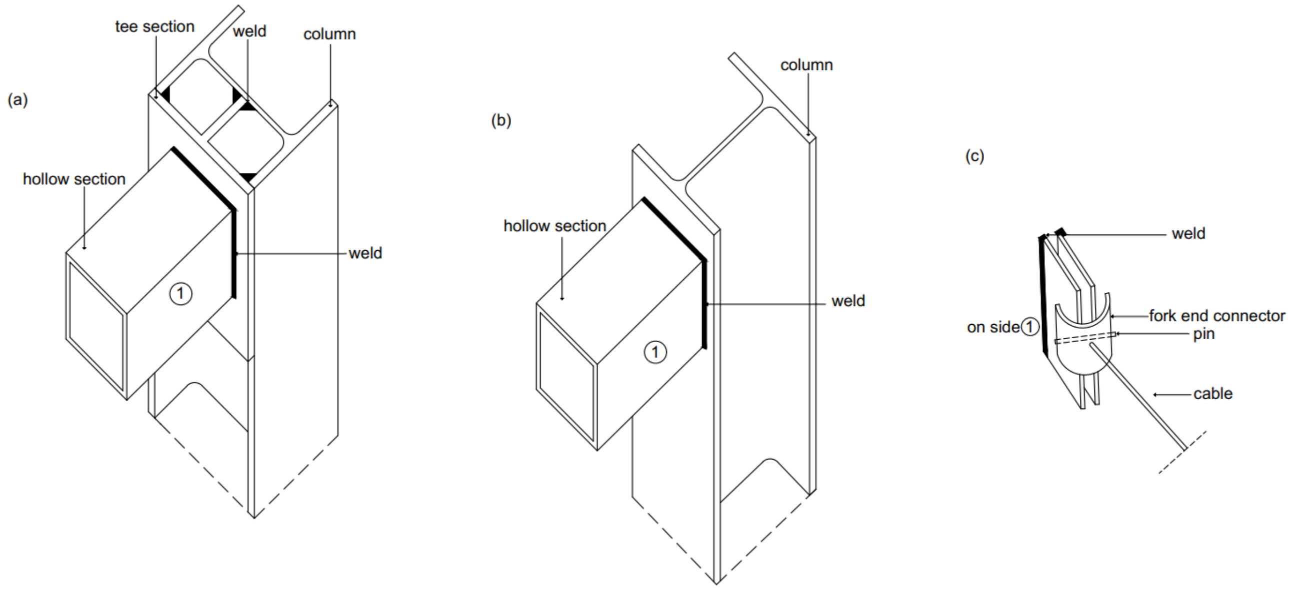

Fig. 12 – Design details for the eccentric implementation of the seesaw system

6. Conclusions

On the basis of the results and discussions presented in the previous sections, it is demonstrated that the seesaw system constitutes an attractive and reliable bracing solution for the seismic design of low-rise steel structures. The spiral strand ropes of the seesaw system are always in tension, thus any buckling issues, as those associated with common steel braces, are eliminated. The details provided can help engineers to design the seesaw system no matter if architectural or structural restrictions may enforce its concentric or eccentric placement with respect to the perimeter frames of a steel structure. It should be also stressed that the seismic response results presented are directly applicable to similar, in terms of symmetry in plan and height and of column orientation, steel structures as those studied herein. Therefore, their generalization to different kinds of steel structures should be investigated.

7. References

[1] Kang JD, Tagawa H (2013): Seismic performance of steel structures with seesaw energy dissipation systems using fluid viscoelastic dampers. *Earthquake Engineering & Structural Dynamics*, **42**, 779-794.

[2] Kang JD, Tagawa H (2013): Seismic performance of steel structures with seesaw energy dissipation systems using fluid viscous dampers, *Engineering Structures*, **56**, 431-442.

[3] Kang JD, Tagawa H (2014): Experimental evaluation of dynamic characteristics of seesaw energy dissipation system for vibration control of structures, *Earthquake Engineering & Structural Dynamics*, **43**, 1889-1995.

[4] Kang JD, Tagawa H (2016): Comparisons between experimental and analytical results for seesaw energy dissipation systems using fluid viscous dampers, Earthquake Engineering & Engineering Vibration, **15**, 79-90.

[5] Katsimpini PS, Papagiannopoulos GA, Sfakianakis MG (2018): On the seismic response and damping capacity of low-rise plane steel frames with seesaw system, *Soil Dynamics & Earthquake Engineering*, **107**, 407-416.

[6] EC3 (2009): *Eurocode 3 - Design of steel structures, Part 1-1: General rules and rules for buildings*, European Committee for Standardization (CEN), Brussels.

[7] EC8 (2009): *Eurocode 8 - Design of structures for earthquake resistance, Part 1-1: General rules, seismic actions and rules for buildings*, European Committee for Standardization (CEN), Brussels.

[8] EC3 (2009): *Eurocode 3 - Design of structures with tension components, Part 1-11: General rules, seismic actions and rules for buildings*, European Committee for Standardization (CEN), Brussels.

[9] SAP 2000 (2016): *Static and dynamic finite element analysis of structures: Version 19.0*, Computers and Structures, Berkeley, California.

[10] Mulliken JS, Karabalis DL (1998): Discrete model for dynamic through-the-soil coupling of 3-d foundations and structures, *Earthquake Engineering & Structural Dynamics*, **27**, 687-710.

[11] ASCE 41-17 (2017): *Seismic evaluation and retrofit of existing buildings*, American Society of Civil Engineers, Virginia, U.S.A.

[12] Boake TM (2014): *Diagrid structures: systems, connections*, details. Birkhäuser.

[13] Ziemian RD (2010): *Guide to stability design criteria for metal structures*. Wiley, 6th Edition.

[14] Kindmann R, Stracke M (2012): *Verbindungen im Stahl- und Verbundbau*. Ernst & Sohn, 3te Auflage.

[15] Petersen C (2013): *Stahlbau*. Springer Verlag, 4te Auflage.

